MINIMAL SURFACE GENERATING FLOW
FOR SPACE CURVES OF NON-VANISHING TORSION

Jiří Minarčík* and Michal Beneš

Department of Mathematics, Faculty of Nuclear Sciences and Physical Engineering
Czech Technical University in Prague
Trojanova 13
Prague, 12000, Czech Republic

(Communicated by Shin-Ichiro Ei)

Abstract. This article introduces new geometric flow for space curves with
positive curvature and torsion. Curves evolving according to this motion law
trace out a zero mean curvature surface. First, the geometry of surfaces defined
as trajectories of moving curves is analyzed and the minimal surface generating
flow is derived. Then, an upper bound for the area of the generated minimal
surface and for the terminating time of the flow is provided.

1. **Introduction.** This article introduces geometric motion law for curves in three-dimensional Euclidean space. In the same way that point mass moving in a homogeneous gravitational field generates parabola, this geometric flow generates a zero mean curvature surface as its trajectory. Studying the trajectory surfaces generated by various geometric flows can yield new insights into the long term behavior of the evolving curves. Conversely, finding geometric flows which generate various types of surfaces may expand our understanding of their geometric and topological properties. Surfaces defined as trajectories of evolving curves were previously studied in [1, 23], where only the special case of inextensible flows has been considered. In this article, we first analyze geometrical properties of surfaces traced out by a general motion law and then discuss the special case of minimal surface generating flow in detail. Several theoretical results explaining the long term behavior of this motion are presented along with upper bound for the area of the generated surface and terminating time for the flow.

In addition to being objects of inherent interest due to their mathematical properties, minimal surfaces have been found useful in many applied fields of research. Starting as a model which describes the shape of soap films spanning a wire frame, zero mean curvature surfaces are now studied in the context of cell membranes [27],

crystallographic structure of zeolites [6, 7, 40] and even general relativity as a representation of the apparent horizon of a black hole [22]. The natural aesthetic of minimal surfaces also serves as an inspiration in architecture and art with examples such as the Olympiastadion in Munich. Recently, the use of periodic minimal surfaces for development of new composite materials have been proposed in [2] and dynamics of soap films with a moving boundary was studied in [20, 19]. Surfaces given by a fixed boundary are also important in knot theory, where the notion of the Seifert surface is associated with a knot invariant called genus (see [44]).

There are several known methods for computation and numerical analysis of minimal surfaces with a prescribed boundary. One of them is the level set method for solving the mean curvature flow of surfaces which converges to a surface of vanishing mean curvature (see e.g. [13, 15]). One can also numerically approximate the Weierstrass-Enneper representation formulas as in [41], use the stretched grid method or utilize the discrete differential geometry approach as discussed in [11, 33, 39, 42].

In this article, we generate minimal surfaces by means of a new geometric flow of curves in space. Space curves evolving according to different motion laws can describe the motion of scroll waves in excitable media [25, 28], dynamics of dislocation loops in crystalline materials [31], evolution of vortex filaments via the localized induction approximation [35] or motion of elastic rods [10]. The classical example of geometric flow of space curves is the curve shortening motion, first considered in [4] and [5]. For recent theoretical results see [3, 14, 21, 26, 30]. The motion law derived in this text involves the torsion of the curve. Geometric flows with torsion were previously considered in [36]. Existence of the solution of related geometric flows was studied in e.g. [18, 16, 24].

The article is organized as follows: Section 2 contains an introduction to general geometric motion of space curves and introduces the notion of trajectory surfaces. The minimal surface generating flow is derived and analyzed in Section 3. The main results contained in this section are the Maximum principle (Proposition 3), upper bound for the generated surface area and for the terminal time (Proposition 5 and Proposition 6, respectively). The section also investigates evolution of global geometric quantities such as the length and the total curvature of the curve. Next is Section 4, which describes the self-similar motion of the helix curve and the generated minimal surface helicoid. This trivial example can be integrated analytically with a solution given in an implicit form.

2. **Trajectory surfaces for general geometric flows.** In this section, we define the necessary notation for the parametric space curves in motion, recall the governing equations for a general geometric flow of curves in $\mathbb{R}^3$ and introduce the notion of trajectory surfaces generated by this general motion law.

Let $\{\Gamma_t\}_{t \in [0, t_{max})}$ denote a family of closed curves in $\mathbb{R}^3$ evolving in time interval $[0, t_{max})$, where $t_{max} > 0$ is the terminal time. For given $t \in [0, t_{max})$, the curve Γ_t is represented by a parametrization $X(\cdot, t): \mathbb{S}^1 \to \mathbb{R}^3$, where $\mathbb{S}^1 = \mathbb{R}/2\pi\mathbb{Z}$ is a unit circle. We use the standard notation for the Frenet frame, i.e. T, N and B denotes the tangent, normal and binormal vector, respectively. The curvature and the torsion, given by the Frenet-Serret formulae, are denoted by κ and τ, respectively. Finally, $g := \|\partial_u X\|$ is the local rate of parametrization and $ds = g\, du$ is the arclength element.

The time evolution of $\{\Gamma_t\}_{t \in [0, t_{max})}$ is given by the geometric flow in the form of the following initial-value problem for the parametrization $X = X(u, t)$:

$$\partial_t X = \beta N + \gamma B \qquad \text{in } \mathbb{S}^1 \times (0, t_{max}), \qquad (1)$$

$$X|_{t=0} = X_0 \qquad \text{in } \mathbb{S}^1, \qquad (2)$$

where X_0 is the parametrization for the initial curve Γ_0. Since the motion in the direction of the tangent vector T does not affect the shape of the curve, we assume zero tangential velocity without any loss of generality.

The evolution equations for the local geometric quantities during the motion given by (1-2) can be retrieved from the general algebraic framework for invariant submanifold flows devised in [32]. According to Example 5.7 from [32], we have

$$\partial_t g = -g\beta\kappa, \qquad (3)$$

$$\partial_t \kappa = \partial_s^2 \beta + \kappa^2 \beta - 2\tau \partial_s \gamma - \gamma \partial_s \tau - \beta \tau^2, \qquad (4)$$

$$\partial_t \tau = 2\beta\kappa\tau + \kappa \partial_s \gamma + \partial_s [\tfrac{1}{\kappa}(\beta \partial_s \tau + 2\tau \partial_s \beta + \partial_s^2 \gamma - \gamma \tau^2)]. \qquad (5)$$

The time evolution of the Frenet frame is given by

$$\partial_t \begin{pmatrix} T \\ N \\ B \end{pmatrix} = \begin{pmatrix} 0 & \partial_s \beta - \gamma\tau & \beta\tau + \partial_s \gamma \\ -\partial_s \beta + \gamma\tau & 0 & \phi \\ -\beta\tau - \partial_s \gamma & -\phi & 0 \end{pmatrix} \cdot \begin{pmatrix} T \\ N \\ B \end{pmatrix}, \qquad (6)$$

where $\phi = \frac{1}{\kappa}(\beta \partial_s \tau + 2\tau \partial_s \beta + \partial_s^2 \gamma - \gamma\tau^2)$.

Definition 2.1 (Trajectory surface). For given velocities β and γ, terminal time t_{max} and an initial curve Γ_0, we define the trajectory surface $\Sigma_{t_{max}}$ as

$$\Sigma_{t_{max}} := \bigcup_{t \in [0, t_{max})} \Gamma_t.$$

Trajectory surfaces have been studied in [23] for the special case of inextensible flows, i.e. geometric flows with $\partial_t g = 0$. An important example of such motion law is the binormal flow, also known as the vortex filament flow or the localized induction approximation, which has applications in the incompressible flows (see e.g. [35]). Surfaces generated by this motion law, referred to as Hasimoto surfaces, have been previously considered in [1]. Another interesting trajectory surface is given in the following example.

Example 1. Simple, spherical curve, moving according to the curve shortening flow ($\beta = \kappa$ and $\gamma = 0$), generates an embedded surface. Moreover, if the curve approaches singularity as t goes to t_{max}, the trajectory surface will be an embedded disc without a point in the center of the original sphere. This is due to the fact that simple spherical curves remain simple and embedded in a shrinking concentric spheres during the curve shortening flow (see [29]).

The first and the second fundamental forms of the surface $\Sigma_{t_{max}}$ generated by (1-2) are given by

$$I \equiv \begin{pmatrix} \mathcal{E} & \mathcal{F} \\ \mathcal{F} & \mathcal{G} \end{pmatrix} = \begin{pmatrix} \|\partial_u X\|^2 & \langle \partial_u X, \partial_t X \rangle \\ \langle \partial_t X, \partial_u X \rangle & \|\partial_t X\|^2 \end{pmatrix},$$

$$II \equiv \begin{pmatrix} \mathcal{L} & \mathcal{M} \\ \mathcal{M} & \mathcal{N} \end{pmatrix} = \begin{pmatrix} \langle \partial_u^2 X, n \rangle & \langle \partial_u \partial_t X, n \rangle \\ \langle \partial_t \partial_u X, n \rangle & \langle \partial_t^2 X, n \rangle \end{pmatrix},$$

where the unit normal vector n of the trajectory surface $\Sigma_{t_{max}}$ can be expressed as

$$n = \|\partial_u X \times \partial_t X\|^{-1} \partial_u X \times \partial_t X = (\beta^2 + \gamma^2)^{-\frac{1}{2}} (\beta B - \gamma N).$$

Using evolution equations (3-6), we obtain the elements of I:

$$\mathcal{E} = g^2, \mathcal{F} = 0 \text{ and } \mathcal{G} = \beta^2 + \gamma^2. \tag{7}$$

Similarly, the elements of the second fundamental form II read

$$\mathcal{L} = -\frac{g^2 \kappa \gamma}{\sqrt{\beta^2 + \gamma^2}}, \quad \mathcal{M} = g \left(\frac{\beta \partial_s \gamma - \gamma \partial_s \beta}{\sqrt{\beta^2 + \gamma^2}} + \tau \sqrt{\beta^2 + \gamma^2} \right),$$

$$\mathcal{N} = \frac{\beta \partial_t \gamma - \gamma \partial_t \beta}{\sqrt{\beta^2 + \gamma^2}} + \frac{\sqrt{\beta^2 + \gamma^2}}{\kappa} (\beta \partial_s \tau + 2\tau \partial_s \beta + \partial_s^2 \gamma - \gamma \tau^2).$$

The Gaussian curvature K and the mean curvature H of $\Sigma_{t_{max}}$ are then computed as

$$K = \frac{\det II}{\det I} = \frac{\mathcal{L}\mathcal{N} - \mathcal{M}^2}{\mathcal{E}\mathcal{G} - \mathcal{F}^2}, \qquad H = \text{Tr}(II(I)^{-1}) = \frac{\mathcal{L}}{\mathcal{E}} + \frac{\mathcal{N}}{\mathcal{G}}.$$

We can write K and H in terms of the functions β, γ, κ and τ as

$$K = \kappa\gamma \frac{\gamma \partial_t \beta - \beta \partial_t \gamma}{(\beta^2 + \gamma^2)^2} - \gamma \frac{\beta \partial_s \tau + 2\tau \partial_s \beta + \partial_s^2 \gamma - \gamma \tau^2}{(\beta^2 + \gamma^2)^{\frac{3}{2}}}$$
$$- \frac{(\beta \partial_s \gamma - \gamma \partial_s \beta)^2}{(\beta^2 + \gamma^2)^2} - 2\tau \frac{\beta \partial_s \gamma - \gamma \partial_s \beta}{\beta^2 + \gamma^2} - \tau^2,$$

$$H = -\frac{\kappa\gamma}{\sqrt{\beta^2 + \gamma^2}} + \frac{\beta \partial_t \gamma - \gamma \partial_t \beta}{(\beta^2 + \gamma^2)^{\frac{3}{2}}} + \frac{\beta \partial_s \tau + 2\tau \partial_s \beta + \partial_s^2 \gamma - \gamma \tau^2}{\kappa \sqrt{\beta^2 + \gamma^2}}.$$

Remark 1. The expressions for K and H significantly simplify if we consider only motion in the normal direction (i.e. $\gamma = 0$):

$$K = -\tau^2, \qquad H = \frac{\beta \partial_s \tau + 2\tau \partial_s \beta}{|\beta| \kappa}. \tag{8}$$

Note that the Gaussian curvature in (8) does not depend on β. Moreover, K is always non-positive and the surface $\Sigma_{t_{max}}$ is developable if and only if the curve Γ_t is evolving in a plane.

3. **Minimal surface generating flow.** This section introduces a new geometric flow for space curves which generates a zero mean curvature surface as its trajectory surface. If the solution to this flow exists for the time long enough, the original curve shrinks to a point leaving us with a minimal surface with boundary given by the initial curve. In this way, the motion can be used as a new method for solving the Plateau's problem.

We restrict the motion by allowing for nonzero velocity in the normal direction only (i.e. $\gamma = 0$) and rewrite the mean curvature of $\Sigma_{t_{max}}$ from (8) as

$$H = \frac{\beta \partial_s \tau + 2\tau \partial_s \beta}{|\beta| \kappa} = \frac{\beta\tau}{|\beta| \kappa} \left(\frac{\partial_s \tau}{\tau} + 2\frac{\partial_s \beta}{\beta} \right) = \frac{\beta\tau}{|\beta| \kappa} \partial_s \left(\log|\tau| + 2\log|\beta| \right).$$

Thus the mean curvature H is zero everywhere, if and only if $\beta = F\tau^{-\frac{1}{2}}$, where $F = F(t)$ is any function independent of the parameter u. We consider the following motion law which generates the minimal surface with the boundary $\partial \Sigma_{t_{max}} = \Gamma_0 \cup \Gamma_{t_{max}}$.

Definition 3.1 (Minimal surface generating flow). Let Γ_0 be a closed space curve with positive curvature and torsion. We say that a family of curves $\{\Gamma_t\}_{t \in [0, t_{max})}$ is evolving according to the Minimal Surface Generating (MSG) flow on the time interval $[0, t_{max})$ if its parametrization X satisfies the following initial value problem:

$$\partial_t X = \tau^{-\frac{1}{2}} N \qquad\qquad \text{in } \mathbb{S}^1 \times (0, t_{max}), \qquad (9)$$

$$X|_{t=0} = X_0 \qquad\qquad \text{in } \mathbb{S}^1, \qquad (10)$$

where X_0 is parametrization of the initial curve Γ_0.

Remark 2. Principal curvatures κ_1 and κ_2 are uniquely determined by K and H as solutions of the quadratic equation $\kappa^2 - 2H\kappa + K = 0$. For $\beta = \tau^{-\frac{1}{2}}$ and $\gamma = 0$, we get $\kappa_{1,2} = \pm\tau$.

For the convenience of the reader, we list the evolution equations for the local geometric quantities derived from (3-5) for the flow (9-10).

$$\partial_t g = -g\kappa\tau^{-\frac{1}{2}}, \qquad (11)$$

$$\partial_t \kappa = \partial_s^2(\tau^{-\frac{1}{2}}) + \tau^{-\frac{1}{2}}(\kappa^2 - \tau^2), \qquad (12)$$

$$\partial_t \tau = 2\kappa\tau^{\frac{1}{2}}. \qquad (13)$$

Similarly, the evolution of the Frenet frame during the flow (9-10) is given by

$$\partial_t \begin{pmatrix} T \\ N \\ B \end{pmatrix} = \begin{pmatrix} 0 & \partial_s(\tau^{-\frac{1}{2}}) & \tau^{\frac{1}{2}} \\ -\partial_s(\tau^{-\frac{1}{2}}) & 0 & 0 \\ -\tau^{\frac{1}{2}} & 0 & 0 \end{pmatrix} \cdot \begin{pmatrix} T \\ N \\ B \end{pmatrix}. \qquad (14)$$

The normal velocity $\beta = \tau^{-\frac{1}{2}}$ is defined only when both $\tau > 0$ and $\kappa > 0$ as the torsion is undefined when $\kappa = 0$. Thus the initial curve must have positive curvature and torsion at all its points. Recently, curves of positive torsion were studied in e.g. [9, 12, 37, 43]. In the next proposition, we show that when the initial curve satisfies this property, the torsion cannot decrease below the original minimal value.

Proposition 1. *Let the initial curve Γ_0 satisfy $\tau > 0$ at all points. Then the torsion τ remains positive for all $t \in (0, t_{max})$. Moreover, the function $\tau(u, t)$ is non-decreasing in time for any fixed $u \in \mathbb{S}^1$.*

Proof. The time derivative of $\sqrt{\tau}$ satisfies

$$\partial_t \sqrt{\tau} = \tfrac{1}{2}\tau^{-\frac{1}{2}}\partial_t\tau = \tfrac{1}{2}\tau^{-\frac{1}{2}}(2\tau^{\frac{1}{2}}\kappa + \partial_s[\tfrac{1}{\kappa}(\tau^{-\frac{1}{2}}\partial_s\tau + 2\tau\partial_s(\tau^{-\frac{1}{2}}))]) = \kappa \geq 0. \qquad (15)$$

From (15) and by the non-negativity of κ, we get

$$\tau(u, t_1) = \left(\sqrt{\tau(u, t_0)} + \int_{t_0}^{t_1} \kappa(u, t)\,\mathrm{d}t\right)^2 \geq \tau(u, t_0)$$

for all $u \in \mathbb{S}^1$ and all $t_0, t_1 \in [0, t_{max})$ such that $t_0 < t_1$. $\qquad\square$

Equation (15) also leads to the following observation, which can be used to validate the results of numerical simulations.

Corollary 1. *The integral of $\sqrt{\tau}$ along the curve Γ_t is preserved.*

Proof. Using formulae (11-14), we have

$$\frac{\mathrm{d}}{\mathrm{d}t} \int_{\Gamma_t} \tau^{\frac{1}{2}}\,\mathrm{d}s = \frac{\mathrm{d}}{\mathrm{d}t} \int_{\mathbb{S}^1} \tau^{\frac{1}{2}} g\,\mathrm{d}u = \int_{\mathbb{S}^1} \partial_t(\tau^{\frac{1}{2}})g + \tau^{\frac{1}{2}}\partial_t g\,\mathrm{d}u = 0.$$

Thus the integral of $\sqrt{\tau}$ remains a positive constant. $\qquad\square$

Since the normal velocity for the MSG flow is always positive, the flow exhibits properties similar to the classical curve shortening flow. These properties are stated in the next two propositions.

Proposition 2. *The length of Γ_t monotonically decreases in time.*

Proof. Using formulae (11-14), we obtain

$$\frac{\mathrm{d}}{\mathrm{d}t}\int_{\Gamma_t}\mathrm{d}s = \int_{\mathbb{S}^1}\partial_t g\,\mathrm{d}u = -\int_{\Gamma_t}\kappa\tau^{-\frac{1}{2}}\,\mathrm{d}s < 0.$$

$\qquad\square$

The following lemma states that the moving curve stays within a cuboid that bounds the initial curve. This property is analogous to the maximum principle for the heat equation.

Lemma 3.2. *Let $\{\Gamma_t\}_{t\in[0,t_{max})}$ be a family of closed curves evolving according to the MSG flow (9-10) with the initial condition Γ_0. For $i = 1, 2, 3$ and $t \in [0, t_{max})$, set*

$$m_i(t) := \min_{u\in\mathbb{S}^1} X_i(u,t) \qquad and \qquad M_i(t) := \max_{u\in\mathbb{S}^1} X_i(u,t),$$

where X_i is the i-th coordinate of X. Then for all $t \in [0, t_{max})$ we have

$$\Gamma_t \subset \underset{i=1}{\overset{3}{\times}}[m_i(0), M_i(0)],$$

where $\times$ denotes the Cartesian product of the indexed intervals.

Proof. Choose any of $i = 1, 2, 3$ and $t \in (0, t_{max})$. Because $\mathbb{S}^1$ is compact and $X(\cdot, t)$ is continuous, the function X_i attains its maximum $M_i(t)$ at some point $u_i^M \in \mathbb{S}^1$. The parametric function then satisfies $\partial_u X_i(u_i^M, t) = 0$ and $\partial_u^2 X_i(u_i^M, t) \leq 0$. Since

$$\partial_t X_i = \tau^{-\frac{1}{2}}N_i = \frac{\|\partial_u X\|\partial_u^2 X_i - \partial_u\|\partial_u X\|\partial_u X_i}{\kappa\tau^{\frac{1}{2}}\|\partial_u X\|^3}$$

and the curvature κ is positive, we have $\partial_t X_i(u_i^M, t) \leq 0$. Similarly, X_i must attain its minimum $m_i(t)$ at some point $u_i^m \in \mathbb{S}^1$ and one can show that $\partial_t X_i(u_i^m, t) \leq 0$ when $X_i(u_i^m, t) = m_i(t)$. Thus

$$m_i(0) \leq m_i(t) \leq M_i(t) \leq M_i(0)$$

for all $t \in [0, t_{max})$ and $i = 1, 2, 3$. $\qquad\square$

Proposition 3. *Let $\{\Gamma_t\}_{t\in[0,t_{max})}$ be a family of closed curves evolving according to the MSG flow (9-10) with the initial condition Γ_0. Then Γ_t lies in the convex hull of the initial curve Γ_0 for all $t \in [0, t_{max})$.*

Proof. The statement is obtained by applying Lemma 3.2 in all possible coordinate systems as the convex hull is an intersection of all cuboids in which the original curve is inscribed. $\qquad\square$

The following lemma contains a useful formula relating important global geometric quantities during the MSG flow. This equation plays a pivotal role in all remaining proofs.

Lemma 3.3. *The total curvature for the curve evolving according to the MSG flow in the time interval $[0, t_{max})$ satisfies*

$$\int_{\Gamma_{t_{max}}} \kappa \, ds - \int_{\Gamma_0} \kappa \, ds = - \int_0^{t_{max}} \int_{\Gamma_t} \tau^{\frac{3}{2}} \, ds \, dt. \tag{16}$$

Proof. The Gauss-Bonnet theorem applied to $\Sigma_{t_{max}}$ states that

$$\int_{\Sigma_{t_{max}}} K \, dA + \int_{\partial \Sigma_{t_{max}}} \kappa_g \, ds = 2\pi \chi(\Sigma_{t_{max}}), \tag{17}$$

where $\partial \Sigma_{t_{max}} = \Gamma_0 \cup \Gamma_{t_{max}}$, κ_g is the geodesic curvature of $\partial \Sigma_{t_{max}}$ and χ is the Euler characteristic. Note that the right-hand-side of (17) vanishes because $\chi(\Sigma_{t_{max}}) = 0$.

The first integral from (17) can be written as

$$\int_{\Sigma_{t_{max}}} K \, dA = \int_0^{t_{max}} \int_{\Gamma_t} K\tau^{-\frac{1}{2}} \, ds \, dt = - \int_0^{t_{max}} \int_{\Gamma_t} \tau^{\frac{3}{2}} \, ds \, dt,$$

because the area element dA can be computed from the first fundamental form as $dA = \sqrt{\mathcal{E}\mathcal{G} - \mathcal{F}^2} \, du \wedge dt = g\tau^{-\frac{1}{2}} \, du \wedge dt$, where $\mathcal{E}$, $\mathcal{G}$ and $\mathcal{F}$ are defined in (7). Since $n = B$ on $\partial \Sigma_{t_{max}}$, the geodesic curvature κ_g satisfies $\kappa_g = \kappa$ on Γ_0 and $\kappa_g = -\kappa$ on $\Gamma_{t_{max}}$. Thus the second integral from (17) can be written as

$$\int_{\partial \Sigma_{t_{max}}} \kappa_g \, ds = \int_{\Gamma_0} \kappa \, ds - \int_{\Gamma_{t_{max}}} \kappa \, ds.$$

By substituting all of the above into (17), we arrive at (16). $\qquad\square$

Equation (16) can also be computed in more straightforward manner by differentiating total curvature and using (11-14), because

$$\frac{d}{dt} \int_{\Gamma_t} \kappa \, ds = \int_{\mathbb{S}^1} \kappa \partial_t \|\partial_u X\| \, du + \int_{\mathbb{S}^1} \partial_t \kappa \|\partial_u X\| \, du$$

$$= - \int_{\Gamma_t} \kappa^2 \tau^{-\frac{1}{2}} \, ds + \int_{\Gamma_t} \partial_s^2(\tau^{-\frac{1}{2}}) + \kappa^2 \tau^{-\frac{1}{2}} - \tau^{\frac{3}{2}} \, ds = - \int_{\Gamma_t} \tau^{\frac{3}{2}} \, ds. \tag{18}$$

In Proposition 2, we show that the curve shrinks in time similarly to the classical curve shortening flow which is in fact a gradient flow minimizing the length functional. Lemma 3.3 allows us to expand this statement and prove that the curve shrinks to a singular point provided the solution exists for the time extend long enough.

Proposition 4. *Let Γ_0 be a closed curve with a finite total curvature and torsion $\tau(u, 0)$ which is defined for all $u \in \mathbb{S}^1$ and satisfies*

$$\inf_{\Gamma_0} \tau := \inf_{u \in \mathbb{S}^1} \tau(u, 0) > 0.$$

If $t_{max} = +\infty$ then Γ_t shrinks to a point as the time t approaches t_{max}.

Proof. Proposition 1 and the assumptions for the initial curve Γ_0 imply

$$\int_0^{t_{max}} \int_{\Gamma_t} \tau^{\frac{3}{2}} \, ds \, dt \geq \int_0^{t_{max}} \inf_{\Gamma_t} \tau^{\frac{3}{2}} \int_{\Gamma_t} ds \, dt \geq \inf_{\Gamma_0} \tau^{\frac{3}{2}} \int_0^{t_{max}} \int_{\Gamma_t} ds \, dt.$$

Using equation (16) and the Fenchel theorem yields

$$\int_0^{t_{max}} \int_{\Gamma_t} \mathrm{d}s \, \mathrm{d}t \leq \frac{1}{\inf_{\Gamma_0} \tau^{\frac{3}{2}}} \left(\int_{\Gamma_0} \kappa \, \mathrm{d}s - \int_{\Gamma_{t_{max}}} \kappa \, \mathrm{d}s \right) \tag{19}$$

$$\leq \frac{1}{\inf_{\Gamma_0} \tau^{\frac{3}{2}}} \left(\int_{\Gamma_0} \kappa \, \mathrm{d}s - 2\pi \right). \tag{20}$$

Since the right-hand side of (20) is finite and it does not depend on t_{max}, the positive integrand $\int_{\Gamma_t} \mathrm{d}s$ must approach 0 as $t \to \infty$. □

Next proposition is one of the main results of this article. It gives us an upper bound for the area swept by the moving curve.

Proposition 5. *Area $A(\Sigma_{t_{max}})$ of the trajectory surface $\Sigma_{t_{max}}$ generated by the flow (9-10) from the initial curve Γ_0 with $\inf_{\Gamma_0} \tau > 0$ satisfies*

$$A(\Sigma_{t_{max}}) \leq \frac{1}{\inf_{\Gamma_0} \tau^2} \left(\int_{\Gamma_0} \kappa \, \mathrm{d}s - 2\pi \right). \tag{21}$$

Proof. From Proposition 1 and inequality (20), we have

$$A(\Sigma_{t_{max}}) = \int_{\Sigma_{t_{max}}} \mathrm{d}A = \int_0^{t_{max}} \int_{\Gamma_t} \tau^{-\frac{1}{2}} \, \mathrm{d}s \, \mathrm{d}t \leq \frac{1}{\inf_{\Gamma_0} \tau^2} \left(\int_{\Gamma_0} \kappa \, \mathrm{d}s - 2\pi \right).$$

□

Note that the upper bound in (21) does not depend on t_{max}. It is computed from geometric properties of the initial curve Γ_0 only. Thus this result can potentially be used for finding a theoretical upper bound for the smallest area of a minimal surface with a prescribed boundary.

The bound may be further improved for initially knotted curves. If the curve would remain knotted, one could use the Milnor-Fary theorem and replace 2π on the right hand side of (21) by 4π.

The goal of the final part of this section is to investigate the long term behavior of curvature and torsion as it dictates the existence of the solution and formation of singularities during the flow (9-10). The analysis of these evolution equations is complicated due to the term $\partial_s^2(\tau^{-\frac{1}{2}})$ in $\partial_t \kappa$. This term vanishes for curves of constant torsion. In order to preserve this property in time, the curve must also have constant curvature. This leads to the trivial example of helix which is discussed in Section 4. Another way to avoid this term is to integrate equations (11-14) along the curve and study the evolution of global quantities such as the averaged curvature $\langle \kappa \rangle$ defined as

$$\langle \kappa(\cdot, t) \rangle := \frac{1}{L(\Gamma_t)} \int_{\Gamma_t} \kappa(s, t) \, \mathrm{d}s, \tag{22}$$

where $L(\Gamma_t)$ is the length of Γ_t. The flow cannot exist when $\langle \kappa \rangle$ vanishes as it implies that κ is zero somewhere along the curve. This approach is explored in the following statement.

Proposition 6. *Let Γ_0 be a closed curve with non-vanishing curvature, torsion satisfying $\tau_0 := \inf_{\Gamma_0} \tau > 0$ and $\langle \kappa(\cdot, 0) \rangle < \tau_0$. Then the MSG flow (9-10) cannot exist beyond the terminal time*

$$t_{max} \leq \frac{1}{2\sqrt{\tau_0}} \log \left(1 + \frac{2 \langle \kappa(\cdot, 0) \rangle}{\tau_0 - \langle \kappa(\cdot, 0) \rangle} \right). \tag{23}$$

Proof. Using formulae (11-14) and (18), we obtain

$$\frac{\mathrm{d}}{\mathrm{d}t}\langle\kappa(\cdot,t)\rangle = -\frac{1}{L(\Gamma_t)}\int_{\Gamma_t}\tau^{\frac{3}{2}}\,\mathrm{d}s + \frac{\langle\kappa(\cdot,t)\rangle}{L(\Gamma_t)}\int_{\Gamma_t}\kappa\tau^{-\frac{1}{2}}\,\mathrm{d}s =: f(\langle\kappa(\cdot,t)\rangle,t). \quad (24)$$

Using equation (22) and Proposition 1, we can bound the right-hand-side as

$$f(\langle\kappa(\cdot,t)\rangle,t) \leq -\inf_{\Gamma_t}\tau^{\frac{3}{2}} + \langle\kappa(\cdot,t)\rangle^2\sup_{\Gamma_t}\tau^{-\frac{1}{2}} \leq \frac{\langle\kappa(\cdot,t)\rangle^2 - \tau_0^2}{\sqrt{\tau_0}} =: g(\langle\kappa(\cdot,t)\rangle).$$

Consider the solution $x = x(t)$ of the initial-value problem $\dot{x}(t) = g(x(t))$, $x(0) = \langle\kappa(\cdot,0)\rangle$ in the form

$$x(t) = -\tau_0\frac{\langle\kappa(\cdot,0)\rangle\cosh(\sqrt{\tau_0}t) - \tau_0\sinh(\sqrt{\tau_0}t)}{\langle\kappa(\cdot,0)\rangle\sinh(\sqrt{\tau_0}t) - \tau_0\cosh(\sqrt{\tau_0}t)}.$$

The solution x monotonically decreases until it reaches zero at the time

$$\tilde{t}_{max} = -\frac{1}{2\sqrt{\tau_0}}\log\left(\frac{\tau_0 - \langle\kappa(\cdot,0)\rangle}{\tau_0 + \langle\kappa(\cdot,0)\rangle}\right).$$

The time derivative of the difference $y(t) := \langle\kappa(\cdot,t)\rangle - x(t)$ can be bounded as

$$\dot{y}(t) = f(\langle\kappa(\cdot,t)\rangle,t) - g(x(t)) \leq g(\langle\kappa(\cdot,t)\rangle) - g(x(t)) = \frac{\langle\kappa(\cdot,t)\rangle + x(t)}{\sqrt{\tau_0}}y(t).$$

From the Grönwall lemma and $y(0) = 0$, we get

$$\langle\kappa(\cdot,t)\rangle = y(t) + x(t) \leq y(0)\exp\left(\int_0^t\frac{\langle\kappa(\cdot,r)\rangle + x(r)}{\sqrt{\tau_0}}\,\mathrm{d}r\right) + x(t) = x(t).$$

Since $x(t)$ is a supersolution of $\langle\kappa(\cdot,t)\rangle$, we have $t_{max} \leq \tilde{t}_{max}$. $\quad\square$

Proposition 6 implies that if the average curvature $\langle\kappa\rangle$ becomes smaller that the infimum of the torsion τ at any time during the flow, the motion will exist only for a finite time bounded by the expression (23). It remains an open question whether this always occurs or whether the flow can exists forever under some circumstances.

4. **Solution of the MSG flow.** Below, we discuss solution of problem (9-10), resp. (11-13). The existence of the solution has not yet been proven. However, an analytical solution in implicit form can be easily obtained for the helix curve.

Example 2 (Helix curve)**.** Evolving helix curve forms the famous minimal surface helicoid. From the symmetries of the helix, we can assume the following shape of the solution for the parametric function X with a given initial condition X_0:

$$X(u,t) := (r(t)\cos u, r(t)\sin u, cu)^T, \qquad X_0(u) := (r_0\cos u, r_0\sin u, cu)^T,$$

where $r_0, c > 0$. As the torsion for the helix is equal to $c(r^2 + c^2)^{-1}$, the problem reduces to an ordinary differential equation $\dot{r}(t) = -(c^{-1}r(t)^2 + c)^{\frac{1}{2}}$ with an implicit solution in form

$$t = -\tfrac{1}{2}c^{\frac{3}{2}}\log\left(c^{-1}r(t) + \left(1 + \left(c^{-1}r(t)\right)^2\right)^{\frac{1}{2}}\right)$$

$$-\tfrac{1}{2}c^{\frac{1}{2}}r(t)\left(1 + \left(c^{-1}r(t)\right)^2\right)^{\frac{1}{2}} + t_{max},$$

where the t_{max} is given by the initial condition r_0. Thus the helix monotonically decreases its radius and asymptotically approaches straight line as the time t tends to t_{max}.
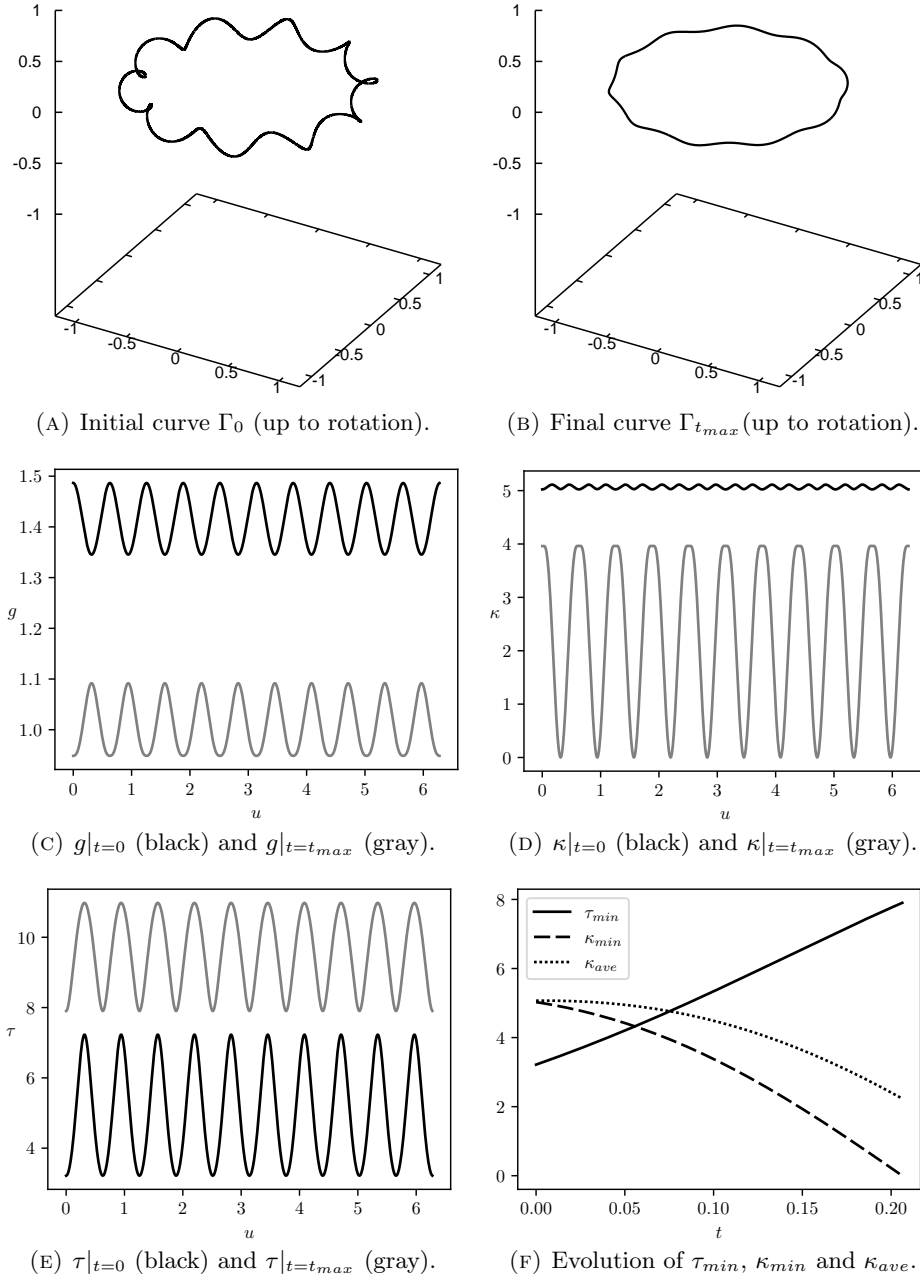
(A) Initial curve Γ_0 (up to rotation).

(B) Final curve $\Gamma_{t_{max}}$ (up to rotation).

(C) $g|_{t=0}$ (black) and $g|_{t=t_{max}}$ (gray).

(D) $\kappa|_{t=0}$ (black) and $\kappa|_{t=t_{max}}$ (gray).

(E) $\tau|_{t=0}$ (black) and $\tau|_{t=t_{max}}$ (gray).

(F) Evolution of τ_{min}, κ_{min} and κ_{ave}.

FIGURE 1. Numerical solution to (11-13) with the initial condition given by (25). The curvature κ vanishes at $t_{max} = 0.20628$. The curves Γ_0 and Γ_{max} were reconstructed from κ, τ and g. The position and orientation was partially recovered using Principal component analysis. However, the rotation around the z-axis was not preserved.

Appendix. We accompany the above mentioned example by a result obtained by means of the numerical approximation. Equations (11-13) have been numerically solved by the explicit Euler first-order method using the finite difference approximations along the parametric interval.

The results presented in Figure 1 show the evolution of closed initial curve with parametrization

$$X_0(u) = (\cos u(r_1 + r_2 \cos(mu)), \sin u(r_1 + r_2 \cos(mu)), r_2 \sin)^T \qquad (25)$$

for all $u \in \mathbb{S}^1$. This specific experiment used parameters $m = 10$, $r_1 = 1$ and $r_2 = \frac{1}{10}$. The initial condition for the values of g, κ and τ was analytically derived from (25). The experiment was run with time step $\Delta t = 10^{-6}$ and the curve was discretized with 10^3 points.

The validity of the numerical results was partially verified by several sanity checks and the numerical scheme was partially validated using the known solution described in Example 2. During the experiment, the integral $\int_{\Gamma_t} \sqrt{\tau}\,\mathrm{d}s$ deviated from its initial value by less then $2 \cdot 10^{-14}$, which is in accordance to Corollary 1. The length was monotonically decreasing (see Proposition 2) while the torsion τ was increasing at every fixed $u \in \mathbb{S}^1$ (see Proposition 1). Even tough, the assumptions for Proposition 6 were not satisfied by the initial configuration, the averaged curvature κ_{ave} eventually became lower than the minimum of torsion τ_{min}. The curvature then vanished after finite time as predicted by Proposition 6.

REFERENCES

[1] N. H. Abdel-All, R. A. Hussien and T. Youssef, Hasimoto Surfaces, *Life Science Journal*, **9** (2012), 556–560.

[2] O. Al-Ketan, R. K. A. Al-Rub and R. Rowshan, Mechanical properties of a new type of architected interpenetrating phase composite materials, *Advanced Materials Technologies*, **2** (2016).

[3] D. J. Altschuler, S. J. Altschuler, S. B. Angenent and L. F. Wu, The zoo of solitons for curve shortening in $\mathbb{R}^n$, *Nonlinearity*, **26** (2013), 1189–1226.

[4] S. J. Altschuler, Singularities for the curve shortening flow for space curves, *Journal of Differential Geometry*, **34** (1991), 491–514.

[5] S. J. Altschuler and M. A. Grayson, Shortening space curves and flow through singularities, *Journal of Differential Geometry*, **35** (1992), 283–298.

[6] S. Andersson, S. T. Hyde and J. O. Bovin, On the periodic minimal surfaces and the conductivity mechanism of α-AgI, *Zeitschrift für Kristallographie*, **173** (1985), 97–99.

[7] S. Andersson, S. T. Hyde, K. Larsson and S. Lidin, Minimal surfaces and structures: From inorganic and metal crystals to cell membranes and biopolymers, *Chemical Reviews*, **88** (1988), 221–242.

[8] J. Arroyo, O. Garay and A. Pampano, Binormal motion of curves with constant torsion in 3-spaces, *Advances in Mathematical Physics*, **2017** (2017), Art. ID 7075831, 8 pp.

[9] L. M. Bates and O. M. Melko, On curves of constant torsion I, *Journal of Geometry*, **104** (2013), 213–227.

[10] M. Bergou, M. Wardetzky, S. Robinson, B. Audoly and E. Grinspun, Discrete elastic rods, *ACM SIGGRAPH*, **63** (2008), 231–264.

[11] A. Bobenko, T. Hoffmann and B. Springborn, Minimal surfaces from circle patterns: Geometry from combinatorics, *Annals of Mathematics*, **164** (2006), 231–264.

[12] H. L. Bray and J. L. Jauregui, On curves with nonnegative torsion, *Archiv der Mathematik*, **104** (2015), 561–575.

[13] D. L. Chopp, Computing minimal surfaces via level set curvature flow, *Journal of Computational Physics*, **106** (1993), 77–91.

[14] K. Corrales, Non existence of type II singularities for embedded and unknotted space curves, preprint, `arXiv:1605.03100v1`, 2016.

[15] G. Dziuk, An algorithm for evolutionary surfaces, *Numerische Mathematik*, **58** (1990), 603–611.

[16] G. Dziuk, E. Kuwert and R. Schätzle, Evolution of elastic curves in $\mathbb{R}^n$: existence and computation, *SIAM Journal on Mathematical Analysis*, **33** (2002), 1228–1245.

[17] M. Erdoğdu and M. Özdemir, Geometry of hasimoto surfaces in minkowski 3-space, *Mathematical Physics, Analysis and Geometry*, **17** (2014), 169–181.

[18] M. Gage and R. S. Hamilton, The heat equation shrinking convex plane curves, *Journal of Differential Geometry*, **23** (1986), 69–96.

[19] R. E. Goldstein, J. McTavish, H. K. Moffatt and A. I. Pesci, Boundary singularities produced by the motion of soap films, *Proceedings of the National Academy of Sciences of the United States of America*, **111** (2014), 8339–8344.

[20] R. E. Goldstein, H. K. Moffatt, A. I. Pesci and R. L. Ricca, Soap-film Möbius strip changes topology with a twist singularity, *Proceedings of the National Academy of Sciences of the United States of America*, **107** (2010), 21979–21984.

[21] S. He, Distance comparison principle and Grayson type theorem in the three dimensional curve shortening flow, preprint, `arXiv:1209.5146v1`, 2012.

[22] G. Huisken and T. Ilmanen, The inverse mean curvature flow and the Riemannian Penrose inequality, *Journal of Differential Geometry*, **59** (2001), 353–437.

[23] R. A. Hussien and S. G. Mohamed, Generated surfaces via inextensible flows of curves in $\mathbb{R}^3$, *Journal of Applied Mathematics*, **2016** (2016), Art. ID 6178961, 8 pp.

[24] T. A. Ivey, Integrable geometric evolution equations for curves, *Contemporary Mathematics*, **285** (2001), 71–84.

[25] J. P. Keener, The dynamics of three-dimensional scroll waves in excitable media, *Physica D*, **31** (1988), 269–276.

[26] G. Khan, A condition ensuring spatial curves develop type-II singularities under curve shortening flow, preprint, `arXiv:1209.4072v3`, 2015.

[27] M. Larsson and K. Larsson, Periodic minimal surface organizations of the lipid bilayer at the lung surface and in cubic cytomembrane assemblies, *Advances in Colloid and Interface Science*, **205** (2014), 68–73.

[28] F. Maucher and P. Sutcliffe, Untangling Knots Via Reaction-Diffusion Dynamics of Vortex Strings, *Physical Review Letters*, **116** (2016), 178101.

[29] J. Minarčík and M. Beneš, Long-term behavior of curve shortening flow in $\mathbb{R}^3$, *SIAM Journal on Mathematical Analysis*, **52** (2020), 1221–1231.

[30] J. Minarčík, M. Kimura and M. Beneš, Comparing motion of curves and hypersurfaces in $\mathbb{R}^m$, *Discrete and Continuous Dynamical Systems-Series B*, **24** (2019), 4815–4826.

[31] T. Mura, *Micromechanics of Defects in Solids*, Springer Netherlands, 1987.

[32] P. J. Olver, Invariant submanifold flows, *Journal of Physics A: Mathematical and Theoretical*, **41** (2008), 344017, 22pp.

[33] U. Pinkall and K. Polthier, Computing discrete minimal surfaces and their conjugates, *Experimental Mathematics*, **2** (1993), 15–36.

[34] H. Pottmann, A. Schiftner and J. Wallner, Geometry of architectural freeform structures, *Internationalen Mathematischen Nachrichten*, **209** (2008), 15–28.

[35] R. L. Ricca, Rediscovery of da Rios equations, *Nature*, **352** (1991), 561–562.

[36] G. Richardson and J. R. King, The evolution of space curves by curvature and torsion, *Journal of Physics A: Mathematical and General*, **35** (2002), 9857–9879.

[37] S. Rodrigues Costa and M. D. C. Romero-Fuster, Nowhere vanishing torsion closed curves always hide twice, *Geometriae Dedicata*, **66** (1997), 1–17.

[38] W. K. Schief and C. Rogers, Binormal motion of curves of constant curvature and torsion. Generation of soliton surfaces, *Proceedings of The Royal Society A-Mathematical Physical and Engineering Sciences*, **455** (1999), 3163–3188.

[39] H. Schumacher and M. Wardetzky, Variational convergence of discrete minimal surfaces, *Numerische Mathematik*, **141** (2019), 173–213.

[40] L. E. Scriven, Equilibrium bicontinuous structure, *Nature*, **263** (1976), 123–125.

[41] H. Terrones, Computation of minimal surfaces, *Journal de Physique Colloques*, **51** (1990), 345–362.

[42] S. Wang and A. Chern, Computing Minimal Surfaces with Differential Forms, *ACM Transactions on Graphics*, **40** (2021), 1–14.

[43] J. L. Weiner, Closed curves of constant torsion. II, *Proceedings of the American Mathematical Society*, **67** (1977), 306–308.

[44] J. J. van Wijk and A. M. Cohen, Visualization of seifert surfaces, *IEEE Trans. on Visualization and Computer Graphics*, **12** (2006), 485–496.

E-mail address: jiri.minarcik@fjfi.cvut.cz
E-mail address: michal.benes@fjfi.cvut.cz